J. Math. Computer Sci., 42 (2026), 64–84

Online: ISSN 2008-949X

Journal of Mathematics and Computer Science

Journal Homepage: www.isr-publications.com/jmcs

Algebraic approaches to solving fractional coupled Navier-Stokes equations

Yousuf Alkhezi[a], Ahmad Shafee[b,*]

[a]Mathematics Department, College of Basic Education, Public Authority for Applied Education and Training (PAAET), Shuwaikh 70654, Kuwait.

[b]PAAET, College of Technological Studies, Laboratory Technology Department, Shuwaikh 70654, Kuwait.

Abstract

The present paper explores the use of the Mohand Variational Iteration Method (MVIM) and q-Homotopy Mohand Transform Method (q-HMTM) to get approximate analytical solutions of the Caputo-type of fractional Navier-Stokes equations. Adaptability of the two methods is evaluated using two different sets of initial conditions. The Mohand transformation allows the fractional derivatives to be treated easily and handle coupled nonlinear terms easily, while the q-HMTM adds an auxiliary parameter that comes to control the convergence of the series solution. Quantitative solutions given both in tables and graphs show that the solutions given by both procedures are in very good agreement with the exact solutions. Comparative analysis shows reliability, stability, and high accuracy of both MVIM and q-HMTM in solving nonlinear coupled fractional PDEs, and outlines the possibilities of the Mohand transformation as an efficient analytical method in fractional fluid dynamics.

Keywords: Fractional order differential equations, system of Navier-Stokes equations, Mohand variational iteration method (MVIM), q-Homotopy Mohand transform method (q-HMTM), Caputo operator.

2020 MSC: 26A33, 32W50, 34A25.

1. Introduction

Fractional calculus (FC) which was originally discovered more than three centuries ago has become increasingly pertinent in recent decades as the power of FC has been discovered by researchers in many different realms of science and engineering. This revival comes mainly because it has the advantages of being able to use memory effects and nonlocal interactions and hereditary properties in mathematical models; all of which are important in modeling complex and heterogeneous systems. FC generalizes the notion of differentiation to arbitrary (non integer) orders and therefore gives an elasticity to mathematics in describing the dynamics of systems that classical calculus cannot explain due to long term temporal correlation or local spatial inhomogeneities [31, 35]. Differential operators of non-integer order have been especially useful in the modeling of anomalous diffusion and transport in complex media, and recent increases in computing capabilities have allowed their successful use to many different fields of science [32, 33, 52]. Permitted applications of FC have been very successful in the fields of biomathematics

*Corresponding author
Email addresses: ya.alkhezi@paaet.edu.kw (Yousuf Alkhezi), as.zada@paaet.edu.kw (Ahmad Shafee)

doi: 10.22436/jmcs.042.01.04

Received: 2025-07-14 *Revised:* 2025-08-14 *Accepted:* 2025-10-24

[12], chaos theory [13], financial mathematics [48], optics [16], and numerous other areas of science and technology [34, 41, 42, 47, 49, 50], highlighting its practical complexity and utility.

Modeling nonlinear systems of partial differential equations (PDEs) has long been a persistent problem in applied mathematics because nonlinearity together with memory effects may result in complex dynamical behavior. In this regard, fractional derivatives open up new possibilities to describe processes in the real world more accurately and flexibly. Much attention has been paid to the types of fractional derivatives, their properties, and the effect that they have on the model behavior [27, 39, 40, 46]. Podlubny [40] summarized some of the many diverse applications that have been realized due to fractional calculus. In epidemiology, as an example, the fractional stochastic susceptible-infective-susceptible (SIS) model of epidemic with low vaccination indicates the value of fractional modeling to reproduce realistic population dynamics. Abuasad et al. [3] also used the fractional multi-step differential transform method to approximate the solutions of this issue, and Ross [44] described the most significant conditions that define the fractional derivatives. The attempts of other researchers to relate two or more methods in order to obtain analytical or numerical solutions have led to different suggestions of new definitions of fractional derivatives as well. As an illustration, variants of the beta fractional derivative have been proposed to obtain an accurate solution of time-fractional diffusion equations in several spatial dimensions [1, 2].

The fractional-order Navier-Stokes (NS) equations constitute an especially important advancement of fluid dynamics within this wider context. It is possible that by using a fractional derivative instead of the traditional time derivative (usually in the Caputo form), the fractional NS equations can bridge between classical and anomalous flows in order to model memory-dependent transport behavior more sensitively. It is the fractional extension that allows many different kinds of flow behavior to be investigated by simply varying the fractional order, and so one can model many kinds of processes between viscoelastic flows and anomalous diffusion in porous media. Notably, this flexibility also makes it possible to adjust the model to better represent data in the experiment or observation, and hence to enhance the predictive accuracy of the solutions as well as their relevance to physical experiments. The present procedures is based on the idea of applying the Mohand transformations in conjunction with the q-Homotopy analysis method and variational iteration method to fractional derivatives in the Caputo sense, so that solutions to the fractional NS system could be reconstructed in terms of different fractional orders. In such a manner, several individual distinct dynamical behaviors of the NS system can be disclosed and explored at the same time.

A number of notable contributions have been made to this field. Herrmann [23] and Hilfer [24] explained the relevance of fractional PDEs in science and engineering, and applications of fractional PDEs in other fields such as the time-fractional NS system. El-Shahed and Salem [19] were the first to model the NS equations in a fractional manner, generalizing the equations through use of Laplace, finite Hankel and finite Fourier sine transformations. Subsequently Kumar et al. [29] analytically solved a nonlinear fractional NS model by coupled with homotopy perturbation method (HPM) and Laplace transform analysis and Ganji et al. [20] and Ragab et al. [43] applied homotopy analysis method (HAM) to nonlinear time-fractional NS system. Momani and Odibat [37] and Birajdar [14] presented Adomian decomposition method (ADM) in fractional NS equations. Chaurasia and Kumar [17] have worked out solutions that employed a combination of the finite Hankel transform and Laplace transform combination, Kumar et al. [28] have obtained analytical solutions by coupling Laplace transform with the ADM. These contributions together serve to illustrate the wide range of semi-analytical and transform based approaches that have been devised to combat the issues that fractional NS systems present.

The variational iteration method (VIM) has the advantage of being simple and general in its implementation among the family of iterative analytical methods. J. H. He was the first to introduce it. It has been used with great success to many nonlinear problems of a wide nature [21, 22]. With time, VIM has been generalized to include integration with other transforms to enable dealing with fractional operators more adequately resulting in the variation iteration transform method (VITM). Although VITM has been used to solve linear fractional differential equations [51] and nonlinear oscillators [11], in this paper, we augment the same by including the Mohand transform in the VIM framework to obtain a solution

method, the Mohand variational iteration method (MVIM) [45]. The use of the Mohand transform has definite advantages over other transforms normally applied in VITM [10]: it makes Caputo-type fractional derivatives easily tractable in algebraic form, evades the pernicious convolution integrals that plague conventional use of Laplace, Sumudu or other type of integral transforms [4, 6–9], and improves ease of formulas expressing the inversion process. This combination augments convergence, simplifies computational complexity and retains nonlinear nature of the original system. In contrast with techniques such as ADM, which require calculation of the Adomian polynomials in a recursive manner [5], or the mesh point method, which limits the achievable accuracy at discrete points [18], the MVIM method exhibits convergent rates to continuous approximation of solutions with only modest overhead. Other extensions like the Shehu decomposition technique [15, 26, 30] have shown that the decomposition methods are flexible, though when the Mohand transform is incorporated into VIM a more effective and efficient strategy is established in finding solutions to nonlinear fractional PDEs as we shall see in the fractional-order Navier-Stokes system treated here.

The analytical power of the q-homotopy Mohand transform method (q-HMTM) in solving fractional PDEs is also outlined in this work. The q-HMTM takes the versatility of the homotopy analysis method and the efficiency of the Mohand transform (MT). Its greatest strength is its capability to quickly build up series of convergent solutions through combining two complementary strategies. Whereas classical integral transforms (like those of Fourier and Laplace) are well studied, MT is a more recent transform whose operations rules are distinct. It is distinguished among other transforms by its property of unity which eases algebraic manipulations of fractional derivatives. In contrast to Laplace and Sumudu transforms which sometimes lead to complicated inverse formulas with Mittag-Leffler functions, the Mohand transform tends to conserve compact recursive form and simpler inversion. Consequently, fractional nonlinear PDEs using MT-based hybrid methods typically have lower computational cost and smaller CPU time. The MT-based combination of the semi-analytical methods VIM, q-homotopy allows simplifying the fractional operators together with fast convergence.

In this paper, q-HMTM and MVIM are applied to the fractional-order NS equations within the framework of the Caputo fractional order derivative. The innovation with regard to this work is use of the Mohand transform as the primary operator that possesses desirable properties compared to the conventional transforms. The numerical experiments typical of the proposed methods performance are provided in details including tables and graphical illustrations that tend to verify the convergence and accuracy of the solution. The comparison between integer-order and fractional-order cases indicate the effects of the fractional parameter and demonstrate the smooth combination of transitions across the regimes of the proposed hybrid methods. Finally, the methods established in this context offer a powerful semi-analytical treatment not just in the context of fractional NS equations but even more general classes of nonlinear fractional PDEs.

2. Concepts of Mohand transform

We will begin by providing an overview of the MT and related ideas in this section.

Definition 2.1. Let consider that $u(t)$ is the function for which the MT is defined by [36] as:

$$M[u(t)] = R(s) = s^2 \int_0^t u(t)e^{-st}dt, \quad k_1 \leqslant s \leqslant k_2.$$

A brief expression of the inverse MT (MIT) is as $M^{-1}[R(s)] = u(t)$.

Definition 2.2 ([38])**.** The MT fractional order derivative is expressed as:

$$M[u^{\psi}(t)] = s^{\psi}R(s) - \sum_{k=0}^{n-1} \frac{u^k(0)}{s^{k-(\psi+1)}}, \ 0 < \psi \leqslant n.$$

Definition 2.3. A few of the characteristics of the MT are given below:

1. $M[u'(t)] = sR(s) - s^2R(0)$;
2. $M[u''(t)] = s^2R(s) - s^3R(0) - s^2R'(0)$;
3. $M[u^n(t)] = s^nR(s) - s^{n+1}R(0) - s^nR'(0) - \cdots - s^nR^{n-1}(0)$.

Lemma 2.4. *Let $u(y,t)$ be an exponentially ordered function. The MT is thus defined as ([25])*

$$M[D_t^{r\psi}u(y,t)] = s^{r\psi}R(s) - \sum_{j=0}^{r-1} s^{\psi(r-j)-1}D_t^{j\psi}u(y,0), \quad 0 < \psi \leqslant 1, \tag{2.1}$$

where $y = (y_1, y_2, \ldots, y_\psi) \in \mathbb{R}^\psi$ and $\psi \in \mathbb{N}$ and $D_t^{r\psi} = D_t^\psi.D_t^\psi.\cdots.D_t^\psi$ (r-times).

Lemma 2.5. *Let us assume that $u(y,t)$ has an exponential order. $M[u(y,t)] = R(s)$ denotes the MT of $u(y,t)$. In relation to the Mohand transform, the multiple fractional power series (MFPS) is written as follows:*

$$R(s) = \sum_{r=0}^{\infty} \frac{\hbar_r(y)}{s^{r\psi+1}}, \quad s > 0,$$

where $y = (s_1, y_2, \ldots, y_\psi) \in \mathbb{R}^\psi$, $\psi \in \mathbb{N}$.

Proof. Consider the Taylor series:

$$u(y,t) = \hbar_0(y) + \hbar_1(y)\frac{t^\psi}{\Gamma[\psi+1]} + +\hbar_2(y)\frac{t^{2\psi}}{\Gamma[2\psi+1]} + \cdots. \tag{2.2}$$

By employing MT on equation (2.2), we obtain the subsequent outcome:

$$M[u(y,t)] = M[\hbar_0(y)] + M\left[\hbar_1(y)\frac{t^\psi}{\Gamma[\psi+1]}\right] + M\left[\hbar_1(y)\frac{t^{2\psi}}{\Gamma[2\psi+1]}\right] + \cdots.$$

The MT features lead to the following result:

$$M[u(y,t)] = \hbar_0(y)\frac{1}{s} + \hbar_1(y)\frac{\Gamma[\psi+1]}{\Gamma[\psi+1]}\frac{1}{s^{\psi+1}} + \hbar_2(y)\frac{\Gamma[2\psi+1]}{\Gamma[2\psi+1]}\frac{1}{s^{2\psi+1}}\cdots.$$

Thus, we get a new Taylor series. □

Lemma 2.6. *Assuming that MT is represented by $M[u(y,t)] = R(s)$, the new Taylor series in MFPS is as follows:*

$$\hbar_0(y) = \lim_{s\to\infty} sR(s) = u(y,0). \tag{2.3}$$

Proof. Assume the Taylor series:

$$\hbar_0(y) = sR(s) - \frac{\hbar_1(y)}{s^\psi} - \frac{\hbar_2(y)}{s^{2\psi}} - \cdots. \tag{2.4}$$

Equation (2.4) is the result of computing and simplifying the limit found in equation (2.3). □

Theorem 2.7. *Consider $M[u(y,t)]$ represents a function. Then, $R(s)$ is denoted in MFPS form as follows:*

$$R(s) = \sum_{r=0}^{\infty} \frac{\hbar_r(y)}{s^{r\psi+1}}, \ s > 0,$$

where $y = (y_1, y_2, \ldots, y_\psi) \in \mathbb{R}^\psi$ and $\psi \in \mathbb{N}$. Then we have $\hbar_r(y) = D_r^{r\psi}u(y,0)$, where $D_t^{r\psi} = D_t^\psi.D_t^\psi.\cdots.D_t^\psi$ (r-times).

Proof. Assume the Taylor series:

$$\hbar_1(y) = s^{\psi+1}R(s) - s^{\psi}\hbar_0(y) - \frac{\hbar_2(y)}{s^{\psi}} - \frac{\hbar_3(y)}{s^{2\psi}} - \cdots . \tag{2.5}$$

The subsequent result is obtained by applying the limit to equation (2.5):

$$\hbar_1(y) = \lim_{s\to\infty}(s^{\psi+1}R(s) - s^{\psi}\hbar_0(y)) - \lim_{s\to\infty}\frac{\hbar_2(y)}{s^{\psi}} - \lim_{s\to\infty}\frac{\hbar_3(y)}{s^{2\psi}} - \cdots .$$

After simplification, we obtain:

$$\hbar_1(y) = \lim_{s\to\infty}(s^{\psi+1}R(s) - s^{\psi}\hbar_0(y)). \tag{2.6}$$

The following version of equation (2.6) can be formed by employing the fundamental concepts delineated in Lemma 2.4:

$$\hbar_1(y) = \lim_{s\to\infty}(sM[D_t^{\psi}u(y,t)](s)). \tag{2.7}$$

The foundation for equation (2.7) is Lemma 2.5:

$$\hbar_1(y) = D_t^{\psi}u(y,0).$$

Again, the Taylor series must be applied and $\lim_{s\to\infty}$ is taken in order to obtain the subsequent outcome,

$$\hbar_2(y) = s^{2\psi+1}R(s) - s^{2\psi}\hbar_0(y) - s^{\psi}\hbar_1(y) - \frac{\hbar_3(y)}{s^{\psi}} - \cdots .$$

Lemma 2.5 is employed to acquire the subsequent outcomes:

$$\hbar_2(y) = \lim_{s\to\infty} s(s^{2\psi}R(s) - s^{2\psi-1}\hbar_0(y) - s^{\psi-1}\hbar_1(y)). \tag{2.8}$$

The equation (2.8) is modified in the following manner, based on Lemmas 2.4 and 2.6:

$$\hbar_2(y) = D_t^{2\psi}u(y,0).$$

The same procedure is followed to obtain the following: $\hbar_3(y) = \lim_{s\to\infty} s(M[D_t^{2\psi}u(y,\psi)](s))$. The final solution is obtained by employing Lemma 2.6 as $\hbar_3(y) = D_t^{3\psi}u(y,0)$. Generally $\hbar_r(y) = D_t^{r\psi}u(y,0)$. So the theorem is proved. □

The following theorem elucidates and describes the novel form of Taylor's series convergence.

Theorem 2.8. *The MFTS expression is characterized by the application of Lemma 2.5, as illustrated:* $M[u(t,y)] = R(s)$. *When* $|s^{a}M[D_t^{(K+1)\psi}u(y,t)]| \leqslant T$, *for all* $s > 0$ *and* $0 < \psi \leqslant 1$, *the residual* $H_K(y,s)$ *of the MFTS satisfies the inequality:*

$$|H_K(y,s)| \leqslant \frac{T}{s^{(K+1)\psi+1}},\ s > 0.$$

Proof. Let $M[D_t^{r\psi}u(y,t)](s)$ is defined on $s > 0$ for $r = 0,1,2,\ldots,K+1$ and consider $|sM[D_{t^{K+1}}u(y,t)]| \leqslant T$. The new Taylor series may be employed to identify the resulting relationship.

$$H_K(y,s) = R(s) - \sum_{r=0}^{K}\frac{\hbar_r(y)}{s^{r\psi+1}}. \tag{2.9}$$

Equation (2.9) and the Theorem 2.7 can be used to obtain the following outcome:

$$H_K(y,s) = R(s) - \sum_{r=0}^{K}\frac{D_t^{r\psi}u(y,0)}{s^{r\psi+1}}. \tag{2.10}$$

In the following step, we multiply $s^{(K+1)\alpha+1}$ with equation (2.10):

$$s^{(K+1)\psi+1}H_K(y,s) = s(s^{(K+1)\psi}R(s) - \sum_{r=0}^{K} s^{(K+1-r)\psi-1}D_t^{r\psi}u(y,0)). \tag{2.11}$$

A new form of equation (2.11) is obtained by using Lemma 2.4:

$$s^{(K+1)\psi+1}H_K(y,s) = sM[D_t^{(K+1)\psi}u(y,t)].$$

Take the absolute:

$$|s^{(K+1)\psi+1}H_K(y,s)| = |sM[D_t^{(K+1)\psi}u(y,t)]|. \tag{2.12}$$

In order to achieve the desired outcome, the condition of equation (2.12) must be implemented,

$$\frac{-T}{s^{(K+1)\psi+1}} \leqslant H_K(y,s) \leqslant \frac{T}{s^{(K+1)\psi+1}}. \tag{2.13}$$

Another way to express the outcome of equation (2.13) is as $|H_K(y,s)| \leqslant \frac{T}{s^{(K+1)\psi+1}}$. Consequently, a distinctive condition for the series' convergence is established. □

3. Methodology

3.1. General methodology of q-HMTM

Let suppose the nonhomogeneous, nonlinear system of PDEs of the fractional order:

$$\begin{aligned} &D_t^{\psi}u_1(y,t) + \mathcal{R}_1u_1(y,t) + \mathcal{N}_1u_1(y,t) = g_1(y,t),\\ &D_t^{\psi}u_2(y,t) + \mathcal{R}_2u_2(y,t) + \mathcal{N}_2u_2(y,t) = g_2(y,t), \quad n-1 < \psi \leqslant n. \end{aligned} \tag{3.1}$$

Here, $D_t^{\psi}u_1(y,t)$ and $D_t^{\psi}u_2(y,t)$ denote the derivative of Caputo, whereas $\mathcal{N}_1$ and $\mathcal{N}_2$ are nonlinear operators and $\mathcal{R}_1$ and $\mathcal{R}_2$ denote the linear operators, and the source terms are $g_1(y,t)$ and $g_2(y,t)$. Subject the Mohand transformation to equation (3.1),

$$\mathcal{M}[u_1(y,t)] - \frac{1}{s^{\psi}}\sum_{k=0}^{n-1} s^{\psi-k-1}{u_1}^k(y,0) + \frac{1}{s^{\psi}}[\mathcal{M}[\mathcal{R}_1u_1(y,t)] + \mathcal{M}[\mathcal{N}_1u_1(y,t)] - \mathcal{M}[g_1(y,t)]] = 0,$$

$$\mathcal{M}[u_2(y,t)] - \frac{1}{s^{\psi}}\sum_{k=0}^{n-1} s^{\psi-k-1}{u_2}^k(y,0) + \frac{1}{s^{\psi}}[\mathcal{M}[\mathcal{R}_2u_2(y,t)] + \mathcal{M}[\mathcal{N}_2u_2(y,t)] - \mathcal{M}[g_2(y,t)]] = 0.$$

The following are the description of the non-linear operators:

$$\begin{aligned} N[\varphi_1(y,t;q)] &= \mathcal{M}[\varphi_1(y,t;q)] - \frac{1}{s^{\psi}}\sum_{k=0}^{n-1} s^{\psi-k-1}{\varphi_1}^k(y,t;q)(0^+)\\ &\quad + \frac{1}{s^{\psi}}[\mathcal{M}[\mathcal{R}_1\varphi_1(y,t;q)] + \mathcal{M}[\mathcal{N}_1\varphi_1(y,t;q)] - \mathcal{M}[g_1(y,t)]],\\ N[\varphi_2(y,t;q)] &= \mathcal{M}[\varphi_2(y,t;q)] - \frac{1}{s^{\psi}}\sum_{k=0}^{n-1} s^{\psi-k-1}{\varphi_2}^k(y,t;q)(0^+)\\ &\quad + \frac{1}{s^{\psi}}[\mathcal{M}[\mathcal{R}_2\varphi_2(y,t;q)] + \mathcal{M}[\mathcal{N}_2\varphi(y,t;q)] - \mathcal{M}[g_2(y,t)]]. \end{aligned}$$

Where the real valued function with respect to y, t, and $q \in \left[0, \frac{1}{n}\right]$ are $\varphi_1(y,t;q))$ and $\varphi_2(y,t;q))$ and defining the homotopy as:

$$\begin{aligned} (1-nq)\mathcal{M}[\varphi_1(y,t;q) - u_{10}(y,t)] &= \hbar q\ \hbar_1(y,t)\mathcal{N}_1[\varphi_1(y,t;q)],\\ (1-nq)\mathcal{M}[\varphi_2(y,t;q) - u_{20}(y,t)] &= \hbar q\ \hbar_2(y,t)\mathcal{N}_2[\varphi_2(y,t;q)]. \end{aligned} \tag{3.2}$$

The auxiliary parameter in the preceding equation is $\hbar = 0$, and the starting conditions are u_{10} and u_{20}.

The following outcomes are true for both $\frac{1}{n}$ and 0:

$$\varphi_1(y,t;0)=u_{10}(y,t),\quad \varphi_1(y,t;\frac{1}{n})=u_1(y,t),\quad \varphi_2(y,t;0)=u_{20}(y,t),\quad \varphi_2(y,t;\frac{1}{n})=u_2(y,t).$$

Due to the intensification of q, the solutions $\varphi_1(y,t;q)$ and $\varphi_2(y,t;q)$ are different from the first estimate $u_{10}(y,t)$ to $u_1(y,t)$ and $u_{20}(y,t)$ to $u_2(y,t)$. The following may be obtained by implementing the Taylor theorem to $\varphi_1(y,t;q)$ and $\varphi_2(y,t;q)$ in relation to q:

$$\varphi_1(y,t;q)=u_{10}(y,t)+\sum_{m=1}^{\infty}u_{1m}(y,t)q^m,\quad \varphi_2(y,t;q)=u_{20}(y,t)+\sum_{m=1}^{\infty}u_{2m}(y,t)q^m,$$

where

$$u_{1m}=\frac{1}{m!}\frac{\partial^m\varphi_1(y,t;q)}{\partial q^m}|_{q=0}\ \text{ and }\ u_{2m}=\frac{1}{m!}\frac{\partial^m\varphi_2(y,t;q)}{\partial q^m}|_{q=0}.$$

For suitable values of $u_{10}(y,t)$, $u_{20}(y,t)$, n, and $\hbar$, the series (3.2) converges at $q=\frac{1}{n}$ and

$$\varphi_1(y,t;q)=u_{10}(y,t)+\sum_{m=1}^{\infty}u_{1m}(y,t)\Big(\frac{1}{n}\Big)^m,\quad \varphi_2(y,t;q)=u_{20}(y,t)+\sum_{m=1}^{\infty}u_{2m}(y,t)\Big(\frac{1}{n}\Big)^m.$$

We calculate the derivative of equation (3.2) with respect to the embedding parameter q by setting $q=0$, and dividing by $m!$:

$$\begin{aligned}\mathcal{M}[u_{1m}(y,t)-k_m u_{1m-1}(y,t)]&=\hbar\mathfrak{h}_1(y,t)\mathcal{R}_{1m}(\overrightarrow{u_1}_{m-1}),\\ \mathcal{M}[u_{2m}(y,t)-k_m u_{2m-1}(y,t)]&=\hbar\mathfrak{h}_2(y,t)\mathcal{R}_{2m}(\overrightarrow{u_2}_{m-1}),\end{aligned}\tag{3.3}$$

Auxiliary parameter $\hbar\neq 0$ and the vectors are defined as follows:

$$\overrightarrow{u_1}_m=[u_{10}(y,t),u_{11}(y,t),\dots,u_{1m}(y,t)],\quad \overrightarrow{u_2}_m=[u_{20}(y,t),u_{21}(y,t),\dots,u_{2m}(y,t)].$$

When equation (3.3) is subjected to the inverse Mohand transform, the following is the result:

$$\begin{aligned}u_{1m}(y,t)&=k_m u_{1m-1}(y,t)+\hbar\mathcal{M}^{-1}[\mathfrak{h}_1(y,t)\mathcal{R}_{1m}(\overrightarrow{u_1}_{m-1})],\\ u_{2m}(y,t)&=k_m u_{2m-1}(y,t)+\hbar\mathcal{M}^{-1}[\mathfrak{h}_2(y,t)\mathcal{R}_{2m}(\overrightarrow{u_2}_{m-1})],\\ \mathcal{R}_{1m}(\overrightarrow{u_1}_{m-1})&=\frac{1}{(m-1)!}\frac{\partial^{m-1}\mathcal{N}_1[\varphi_1(y,t;q)]}{\partial q^{m-1}}|_{q=0},\\ \mathcal{R}_{2m}(\overrightarrow{u_2}_{m-1})&=\frac{1}{(m-1)!}\frac{\partial^{m-1}\mathcal{N}_2[\varphi_2(y,t;q)]}{\partial q^{m-1}}|_{q=0},\\ k_m&=\begin{cases}0, & \text{if } m\leqslant 1,\\ 1, & \text{if } m>1.\end{cases}\end{aligned}\tag{3.4}$$

Equation (3.4) must be solved in order to ascertain the components of the q-HMTM solution.

3.2. General methodology of MVIM

Let suppose the nonhomogeneous, nonlinear system of PDEs of the fractional order:

$$\begin{aligned}D_t^{\psi}u_1(y,t)&=\mathcal{R}_1u_1(y,t)+\mathcal{N}_1u_1(y,t)+g_1(y,t),\\ D_t^{\psi}u_2(y,t)&=\mathcal{R}_2u_2(y,t)+\mathcal{N}_2u_2(y,t)+g_2(y,t),\quad n-1<\psi\leqslant n.\end{aligned}\tag{3.5}$$

Initial conditions are $u_1(y,0) = u_{1n-1}(y)$, $u_2(y,0) = u_{2n-1}(y)$. By using the Mohand transform on equation (3.5), the subsequent outcome is achieved:

$$\begin{aligned}\mathcal{M}[D_t^{\psi} u_1(y,t)] &= \mathcal{M}[\mathcal{R}_1 u_1(y,t) + \mathcal{N} u_1(y,t) + g_1(y,t)],\\ \mathcal{M}[D_t^{\psi} u_2(y,t)] &= \mathcal{M}[\mathcal{R}_2 u_2(y,t) + \mathcal{N} u_2(y,t) + g_2(y,t)].\end{aligned}$$

Using the transform's iteration property, we achieve the following outcome:

$$\begin{aligned}\mathcal{M}[u_1(y,t)] - \sum_{k=0}^{m-1} s^{\psi-k-1} \frac{\partial^k u_1(y,t)}{\partial t^k}|_{t=0} &= \mathcal{M}[\mathcal{R}_1 u_1(y,t) + \mathcal{N}_1 u_1(y,t) + g_1(y,t)],\\ \mathcal{M}[u_2(y,t)] - \sum_{k=0}^{m-1} s^{\psi-k-1} \frac{\partial^k u_2(y,t)}{\partial t^k}|_{t=0} &= \mathcal{M}[\mathcal{R}_2 u_2(y,t) + \mathcal{N}_2 u_2(y,t) + g_2(y,t)].\end{aligned} \tag{3.6}$$

The Lagrange multiplier $(-\lambda(s))$ is integrated iteratively to obtain:

$$\begin{aligned}\mathcal{M}[u_{1n+1}(y,t)] &= \mathcal{M}[u_{1n}(y,t)] - \lambda(s)\Big[\mathcal{M}[u_{1n}(y,t)] - \sum_{k=0}^{m-1} s^{\psi-k-1} \frac{\partial^k u_1(y,0)}{\partial t^k}\Big],\\ \mathcal{M}[u_{2n+1}(y,t)] &= \mathcal{M}[u_{2n}(y,t)] - \lambda(s)\Big[\mathcal{M}[u_{2n}(y,t)] - \sum_{k=0}^{m-1} s^{\psi-k-1} \frac{\partial^k u_2(y,0)}{\partial t^k}\Big].\end{aligned} \tag{3.7}$$

Equation (3.7) is substituted into equation (3.6) provided that $\lambda(s) = -\frac{1}{s^{\psi}}$,

$$\begin{aligned}\mathcal{M}[u_{1n+1}(y,t)] &= \mathcal{M}[u_{1n}(y,t)] - \lambda(s)\Big[\mathcal{M}[u_{1n}(y,t)]\\ &\quad - \sum_{k=0}^{m-1} s^{\psi-k-1} \frac{\partial^k u_1(y,0)}{\partial t^k} + \mathcal{M}[\mathcal{R}_1 u_1(y,t) + \mathcal{N}_1 u_1(y,t) + g_1(y,t)]\Big],\\ \mathcal{M}[u_{2n+1}(y,t)] &= \mathcal{M}[u_{2n}(y,t)] - \lambda(s)\Big[\mathcal{M}[u_{2n}(y,t)]\\ &\quad - \sum_{k=0}^{m-1} s^{\psi-k-1} \frac{\partial^k u_2(y,0)}{\partial t^k} + \mathcal{M}[\mathcal{R}_2 u_2(y,t) + \mathcal{N}_2 u_2(y,t) + g_2(y,t)]\Big],\end{aligned} \tag{3.8}$$

We may obtain the following by applying the Mohand inverse transform on equation (3.8):

$$\begin{aligned}u_{1n+1}(y,t) &= u_{1n}(y,t) + \mathcal{M}^{-1}\Big[\frac{1}{s^{\psi}} \sum_{k=0}^{m-1} s^{\psi-k-1} \frac{\partial^k u_1(y,0)}{\partial t^k} + \mathcal{M}[\mathcal{R}_1 u_1(y,t) + \mathcal{N}_1 u_1(y,t) + g_1(y,t)]\Big],\\ u_{2n+1}(y,t) &= u_{2n}(y,t) + \mathcal{M}^{-1}\Big[\frac{1}{s^{\psi}} \sum_{k=0}^{m-1} s^{\psi-k-1} \frac{\partial^k u_2(y,0)}{\partial t^k} + \mathcal{M}[\mathcal{R}_2 u_2(y,t) + \mathcal{N}_2 u_2(y,t) + g_2(y,t)]\Big].\end{aligned}$$

We get the initial conditions as:

$$u_{10}(y,t) = \mathcal{M}^{-1}\Big[\frac{1}{s^{\psi}} \sum_{k=0}^{m-1} s^{\psi-k-1} \frac{\partial^k u_1(y,0)}{\partial t^k}\Big], \quad u_{20}(y,t) = \mathcal{M}^{-1}\Big[\frac{1}{s^{\psi}} \sum_{k=0}^{m-1} s^{\psi-k-1} \frac{\partial^k u_2(y,0)}{\partial t^k}\Big].$$

The iterative scheme is given as:

$$\begin{aligned}u_{1n+1}(y,t) &= u_{1n}(y,t) + \mathcal{M}^{-1}\Big[\frac{1}{s^{\psi}} \sum_{k=0}^{m-1} s^{\psi-k-1} \frac{\partial^k u_1(y,0)}{\partial t^k} + \mathcal{M}[\mathcal{R}_1 u_1(y,t) + \mathcal{N}_1 u_1(y,t) + g_1(y,t)]\Big],\\ u_{2n+1}(y,t) &= u_{2n}(y,t) + \mathcal{M}^{-1}\Big[\frac{1}{s^{\psi}} \sum_{k=0}^{m-1} s^{\psi-k-1} \frac{\partial^k u_2(y,0)}{\partial t^k} + \mathcal{M}[\mathcal{R}_2 u_2(y,t) + \mathcal{N}_2 u_2(y,t) + g_2(y,t)]\Big].\end{aligned} \tag{3.9}$$

4. Numerical example 1

4.1. Utilization of q*-HMTM*

Assume the NS equation of time fractional order:

$$\begin{aligned} D_t^{\psi} u_1 - a\frac{\partial^2 u_1}{\partial y^2} - a\frac{\partial^2 u_1}{\partial z^2} + u_2\frac{\partial u_1}{\partial z} + u_1\frac{\partial u_1}{\partial y} - q = 0, \\ D_t^{\psi} u_2 - a\frac{\partial^2 u_2}{\partial y^2} - a\frac{\partial^2 u_2}{\partial z^2} + u_1\frac{\partial u_2}{\partial y} + u_2\frac{\partial u_2}{\partial z} + q = 0, \end{aligned} \tag{4.1}$$

where $0 < \psi \leqslant 1$. IC's are given as:

$$\begin{aligned} u_1(y,z,0) &= -e^{y+z}, \\ u_2(y,z,0) &= e^{y+z}, \\ \mathcal{M}[u_1] - s\left(e^{y+z}\right) + \frac{1}{s^{\psi}}\mathcal{M}\Big[- a\frac{\partial^2 u_1}{\partial y^2} - a\frac{\partial^2 u_1}{\partial z^2} + u_2\frac{\partial u_1}{\partial z} + u_1\frac{\partial u_1}{\partial y} - q\Big] &= 0, \\ \mathcal{M}[u_2] + s\left(e^{y+z}\right) + \frac{1}{s^{\psi}}\mathcal{M}\Big[- a\frac{\partial^2 u_2}{\partial y^2} - a\frac{\partial^2 u_2}{\partial z^2} + u_1\frac{\partial u_2}{\partial y} + u_2\frac{\partial u_2}{\partial z} + q\Big] &= 0. \end{aligned}$$

The non-linear operator is defined as:

$$\begin{aligned} &\mathcal{N}^1[\varphi_1(y,z,t;q), \varphi_2(y,z,t;q)] \\ &\quad = \mathcal{M}[\varphi_1(y,z,t;q)] - s\left(e^{y+z}\right) + \frac{1}{s^{\psi}}\mathcal{M}\Big[- a\frac{\partial^2 \varphi_1(y,z,t;q)}{\partial y^2} \\ &\qquad - a\frac{\partial^2 \varphi_1(y,z,t;q)}{\partial z^2} + \varphi_2(y,z,t;q)\frac{\partial \varphi_1(y,z,t;q)}{\partial z} + \varphi_1(y,z,t;q)\frac{\partial \varphi_1(y,z,t;q)}{\partial y} - q\Big], \\ &\mathcal{N}^2[\varphi_1(y,z,t;q), \varphi_2(y,z,t;q)] \\ &\quad = \mathcal{M}[\varphi_2(y,z,t;q)] + s\left(e^{y+z}\right) + \frac{1}{s^{\psi}}\mathcal{M}\Big[- a\frac{\partial^2 \varphi_2(y,z,t;q)}{\partial y^2} \\ &\qquad - a\frac{\partial^2 \varphi_2(y,z,t;q)}{\partial z^2} + \varphi_1(y,z,t;q)\frac{\partial \varphi_2(y,z,t;q)}{\partial y} + \varphi_2(y,z,t;q)\frac{\partial \varphi_2(y,z,t;q)}{\partial z} + q\Big]. \end{aligned}$$

The Mohand operator is define as:

$$\begin{aligned} \mathcal{M}[u_{1m} - k_m u_{1m-1}] &= \hbar\, h(y,z,t)\mathcal{R}_{1,m}[\overrightarrow{u_1}_{m-1}, \overrightarrow{u_2}_{m-1}], \\ \mathcal{M}[u_{2m} - k_m u_{2m-1}] &= \hbar\, h(y,z,t)\mathcal{R}_{2,m}[\overrightarrow{u_1}_{m-1}, \overrightarrow{u_2}_{m-1}]. \end{aligned}$$

Here,

$$\begin{aligned} \mathcal{R}_{1,m}[\overrightarrow{u_1}_{m-1}, \overrightarrow{u_2}_{m-1}] &= \mathcal{M}[u_{1m-1}] - s\left(1 - \frac{k_m}{n}\right)\left(e^{y+z}\right) + \frac{1}{s^{\psi}}\mathcal{M}\Big[- a\frac{\partial^2 u_{1m-1}}{\partial y^2} \\ &\quad - a\frac{\partial^2 u_{1m-1}}{\partial z^2} + \sum_{i=0}^{m-1} u_{2i}\frac{\partial u_{1m-1-i}}{\partial z} + \sum_{i=0}^{m-1} u_{1i}\frac{\partial u_{1m-1-i}}{\partial y} - q\Big], \\ \mathcal{R}_{2,m}[\overrightarrow{u_1}_{m-1}, \overrightarrow{u_2}_{m-1}] &= \mathcal{M}[u_{2m-1}] + s\left(1 - \frac{k_m}{n}\right)\left(e^{y+z}\right) + \frac{1}{s^{\psi}}\mathcal{M}\Big[- a\frac{\partial^2 u_{2m-1}}{\partial y^2} \\ &\quad - a\frac{\partial^2 u_{2m-1}}{\partial z^2} + \sum_{i=0}^{m-1} u_{1i}\frac{\partial u_{2m-1-i}}{\partial y} + \sum_{i=0}^{m-1} u_{2i}\frac{\partial u_{2m-1-i}}{\partial z} + q\Big], \end{aligned}$$

$$\begin{aligned} u_{1m} &= k_m u_{1m-1} + \hbar \mathcal{M}^{-1}[\mathfrak{h}(y,z,t)\mathcal{R}_{1,m}(\overrightarrow{u_1}_{m-1}, \overrightarrow{u_2}_{m-1}), \\ u_{2m} &= k_m u_{2m-1} + \hbar \mathcal{M}^{-1}[\mathfrak{h}(y,z,t)\mathcal{R}_{2,m}(\overrightarrow{u_1}_{m-1}, \overrightarrow{u_2}_{m-1}). \end{aligned} \tag{4.2}$$

With the help of initial condition (4.2) we obtain the subsequent outcome:

$$u_{11} = \frac{\hbar t^{\psi}\left(2ae^{y+z} - q\right)}{\Gamma(\psi+1)}, \qquad u_{21} = \frac{\hbar t^{\alpha}\left(q - 2ae^{y+\psi}\right)}{\Gamma(\psi+1)},$$

$$u_{12} = \hbar t^{\psi}\left(\frac{(n+\hbar)\left(2ae^{y+z} - q\right)}{\Gamma(\psi+1)} - \frac{4a^2\hbar t^{\psi}e^{y+z}}{\Gamma(2\psi+1)}\right), \quad u_{22} = \hbar t^{\psi}\left(\frac{4a^2\hbar t^{\psi}e^{y+z}}{\Gamma(2\psi+1)} + \frac{(n+\hbar)\left(q - 2ae^{y+z}\right)}{\Gamma(\psi+1)}\right),$$

and so on. The solution of equation (4.1), as determined by q-HMTM, is as follows:

$$u_1 = u_{10} + \sum_{m=1}^{\infty} u_{1m}\left(\frac{1}{n}\right)^m, \quad u_2 = u_{20} + \sum_{m=1}^{\infty} u_{2m}\left(\frac{1}{n}\right)^m.$$

For $\psi = 1$, $\hbar = -1$, and $n = 1$ solutions $\sum_{m=1}^{N} u_{1m}\left(\frac{1}{n}\right)^m$ and $\sum_{m=1}^{N} u_{2m}\left(\frac{1}{n}\right)^m$ converge to the exact solutions as $N \to \infty$,

$$u_1(y,z,t) = -e^{y+z} + \frac{\hbar t^{\psi}\left(2ae^{y+z} - q\right)}{\Gamma(\psi+1)} + \hbar t^{\psi}\left(\frac{(n+\hbar)\left(2ae^{y+z} - q\right)}{\Gamma(\psi+1)} - \frac{4a^2\hbar t^{\psi}e^{y+z}}{\Gamma(2\psi+1)}\right) + \cdots = -e^{2at+y+z},$$

$$u_2(y,z,t) = e^{y+z} + \frac{\hbar t^{\alpha}\left(q - 2ae^{y+\psi}\right)}{\Gamma(\psi+1)} + \hbar t^{\psi}\left(\frac{4a^2\hbar t^{\psi}e^{y+z}}{\Gamma(2\psi+1)} + \frac{(n+\hbar)\left(q - 2ae^{y+z}\right)}{\Gamma(\psi+1)}\right) + \cdots = e^{2at+y+z}.$$

4.2. Utilization of MVIM

Assume the NS equation of time fractional order:

$$D_t^{\psi}u_1 = a\frac{\partial^2 u_1}{\partial y^2} + a\frac{\partial^2 u_1}{\partial z^2} - u_2\frac{\partial u_1}{\partial z} - u_1\frac{\partial u_1}{\partial y} - q, \quad D_t^{\psi}u_2 = a\frac{\partial^2 u_2}{\partial y^2} + a\frac{\partial^2 u_2}{\partial z^2} - u_1\frac{\partial u_2}{\partial y} - u_2\frac{\partial u_2}{\partial z} + q,$$

where $0 < \psi \leqslant 1$. IC's are given as: $u_1(y,z,0) = -e^{y+z}$, $u_2(y,z,0) = e^{y+z}$. Using the iterative formula found in equation (3.9), we can obtain

$$u_{1n+1} = u_{1n} + \mathcal{M}^{-1}\Big[\frac{1}{s^{\psi}}\sum_{k=0}^{m-1} s^{\psi-k-1}\frac{\partial^k u_1(y,z,0)}{\partial t^k} + \mathcal{M}[a\frac{\partial^2 u_{1n}}{\partial y^2} + a\frac{\partial^2 u_{1n}}{\partial z^2} - u_{2n}\frac{\partial u_{1n}}{\partial z} - u_{1n}\frac{\partial u_{1n}}{\partial y} - q]\Big],$$

$$u_{2n+1} = u_{2n} + \mathcal{M}^{-1}\Big[\frac{1}{s^{\psi}}\sum_{k=0}^{m-1} s^{\psi-k-1}\frac{\partial^k u_2(y,z,0)}{\partial t^k} + \mathcal{M}[a\frac{\partial^2 u_{2n}}{\partial y^2} + a\frac{\partial^2 u_{2n}}{\partial z^2} - u_{1n}\frac{\partial u_{2n}}{\partial y} - u_{2n}\frac{\partial u_{2n}}{\partial z} + q]\Big].$$

Inserting $n = 0$ into the expression above results in the second approximation:

$$u_{11} = u_{10} + \mathcal{M}^{-1}\Big[\frac{1}{s^{\psi}}\sum_{k=0}^{m-1} s^{\psi-k-1}\frac{\partial^k u_1(y,z,0)}{\partial t^k} + \mathcal{M}[a\frac{\partial^2 u_{10}}{\partial y^2} + a\frac{\partial^2 u_{10}}{\partial z^2} - u_{20}\frac{\partial u_{10}}{\partial z} - u_{10}\frac{\partial u_{10}}{\partial y} - q]\Big],$$

$$u_{21} = u_{20} + \mathcal{M}^{-1}\Big[\frac{1}{s^{\psi}}\sum_{k=0}^{m-1} s^{\psi-k-1}\frac{\partial^k u_2(y,z,0)}{\partial t^k} + \mathcal{M}[a\frac{\partial^2 u_{20}}{\partial y^2} + a\frac{\partial^2 u_{20}}{\partial z^2} - u_{10}\frac{\partial u_{20}}{\partial y} - u_{20}\frac{\partial u_{20}}{\partial z} + q]\Big].$$

By simplification, we get

$$u_{11} = \frac{-2at^{\psi}e^{y+z} + qt^{\psi} - \Gamma(\psi+1)e^{y+z}}{\Gamma(\psi+1)}, \quad u_{21} = \frac{2at^{\psi}e^{y+z} - qt^{\psi} + \Gamma(\psi+1)e^{y+z}}{\Gamma(\psi+1)}.$$

By inserting $n = 1$, we have

$$u_{12} = u_{11} + \mathcal{M}^{-1}\Big[\frac{1}{s^{\psi}}\sum_{k=0}^{m-1} s^{\psi-k-1}\frac{\partial^k u_1(y,z,0)}{\partial t^k} + \mathcal{M}[a\frac{\partial^2 u_{11}}{\partial y^2} + a\frac{\partial^2 u_{11}}{\partial z^2} - u_{21}\frac{\partial u_{11}}{\partial z} - u_{11}\frac{\partial u_{11}}{\partial y} - q]\Big],$$

$$u_{22} = u_{21} + \mathcal{M}^{-1}\Big[\frac{1}{s^{\psi}}\sum_{k=0}^{m-1} s^{\psi-k-1}\frac{\partial^k u_2(y,z,0)}{\partial t^k} + \mathcal{M}[a\frac{\partial^2 u_{21}}{\partial y^2} + a\frac{\partial^2 u_{21}}{\partial z^2} - u_{11}\frac{\partial u_{21}}{\partial y} - u_{21}\frac{\partial u_{21}}{\partial z} + q]\Big].$$

By simplifying the expression, we achieve the subsequent final outcome:

$$u_{12}(y,z,t) = -e^{y+z} - \frac{2at^{\psi}e^{y+z}}{\Gamma(\psi+1)} + \frac{qt^{\psi}}{\Gamma(\psi+1)} - \frac{4a^2t^{2\psi}e^{y+z}}{\Gamma(2\psi+1)},$$

$$u_{22}(y,z,t) = e^{y+z} + \frac{2at^{\psi}e^{y+z}}{\Gamma(\psi+1)} - \frac{qt^{\psi}}{\Gamma(\psi+1)} + \frac{4a^2t^{2\psi}e^{y+z}}{\Gamma(2\psi+1)}.$$

Table 1: q-HMTM and MVIM solution error comparison of $u_1(y,z,t)$ at $z = 0.1$ and $\hbar = -1$.

t	y	MVIM$_{\psi=0.6}$	q-HMTM$_{\psi=0.6}$	MVIM$_{\psi=1}$	q-HMTM$_{\psi=1}$	Exact	MVIM Error$_{\psi=1}$	q-HMTM Error$_{\psi=1}$
	-1.0	-0.408865	-0.408865	-0.407384	-0.407384	-0.407384	5.423639×10^{-10}	5.423640×10^{-10}
	-0.5	-0.674104	-0.674104	-0.671662	-0.671662	-0.671662	8.942070×10^{-10}	8.942071×10^{-10}
0.1	0.0	-1.111410	-1.111410	-1.107380	-1.107380	-1.107380	1.474298×10^{-9}	1.474298×10^{-9}
	0.5	-1.832410	-1.832410	-1.825770	-1.825770	-1.825770	2.430706×10^{-9}	2.430706×10^{-9}
	1.0	-3.021130	-3.021130	-3.010180	-3.010180	-3.010180	4.007557×10^{-9}	4.007558×10^{-9}
	-1.0	-0.412638	-0.412638	-0.410656	-0.410656	-0.410656	6.793135×10^{-8}	6.793135×10^{-8}
	-0.5	-0.680325	-0.680325	-0.677057	-0.677057	-0.677057	1.119998×10^{-7}	1.119998×10^{-7}
0.5	0.0	-1.121670	-1.121670	-1.116280	-1.116280	-1.116280	1.846565×10^{-7}	1.846565×10^{-7}
	0.5	-1.849320	-1.849320	-1.840430	-1.840430	-1.840430	3.044472×10^{-7}	3.044472×10^{-7}
	1.0	-3.049010	-3.049010	-3.034360	-3.034360	-3.034360	5.019485×10^{-7}	5.019485×10^{-7}
	-1.	-0.4158180	-0.415818	-0.414782	-0.414782	-0.414783	5.448142×10^{-7}	5.448142×10^{-7}
	-0.5	-0.685568	-0.685568	-0.683861	-0.683861	-0.683861	8.982467×10^{-7}	8.982467×10^{-7}
1.0	0.0	-1.130310	-1.130310	-1.127500	-1.127500	-1.127500	1.480958×10^{-6}	1.480958×10^{-6}
	0.5	-1.863570	-1.863570	-1.858930	-1.858930	-1.858930	2.441687×10^{-6}	2.441687×10^{-6}
	1.0	-3.072500	-3.072500	-3.064850	-3.064850	-3.064850	4.025662×10^{-6}	4.025662×10^{-6}

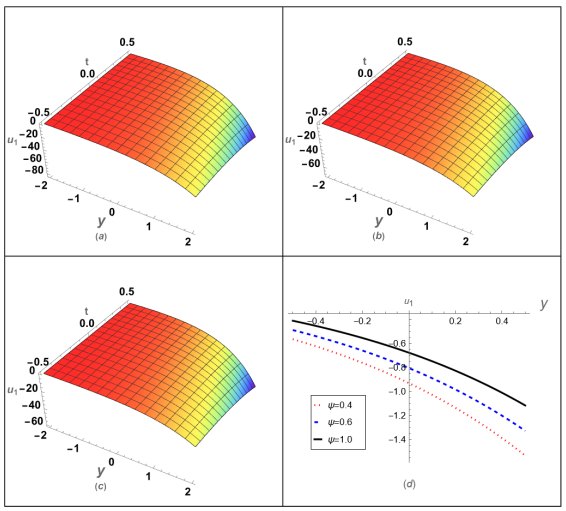

Figure 1: Effect of fractional order, (a) $\psi = 0.4$, (b) $\psi = 0.6$, (c) $\psi = 1.0$ on the approximate solution and (d) comparison of fractional order ψ of the solution $u_1(y,z,t)$ at $t = 1$, $\hbar = -1$, and $z = 0.1$.

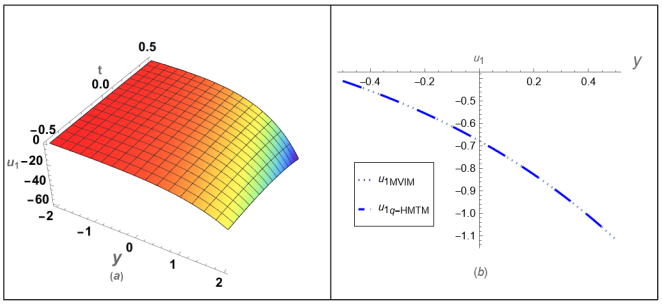

Figure 2: Comparison among MVIM and q-HMTM solution $u_1(y,z,t)$ at $t = 1$, $\hbar = -1$, and $z = 0.1$.

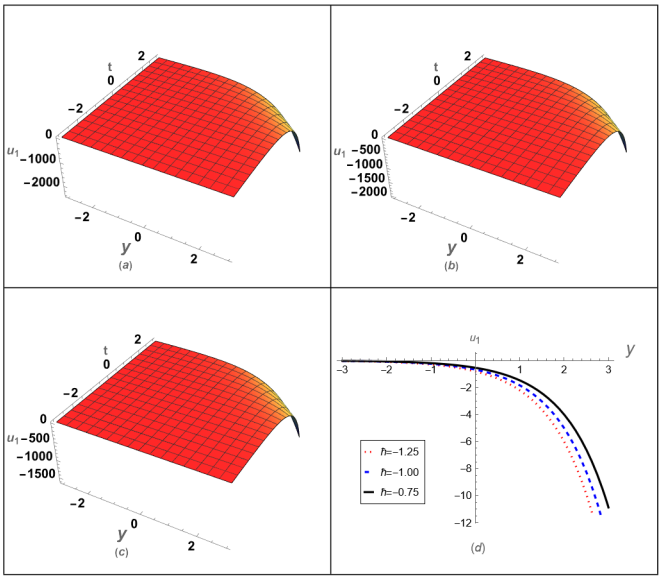

Figure 3: Effect of the auxiliary parameter, (a) $\hbar = -1.25$, (b) $\hbar = -1$, (c) $\hbar = -0.75$ on the approximate solution $u_1(y,z,t)$ at $t = 1$ and $z = 0.1$.

Table 2: q-HMTM and MVIM solution error comparison of $u_2(y,z,t)$ at $z = 0.1$ and $\hbar = -1$.

t	y	$MVIM_{\psi=0.6}$	$q\text{-}HMTM_{\psi=0.6}$	$MVIM_{\psi=1}$	$q\text{-}HMTM_{\psi=1}$	Exact	$MVIM\ Error_{\psi=1}$	$q\text{-}HMTM\ Error_{\psi=1}$
	-1.0	0.408865	0.408865	0.407384	0.407384	0.407384	5.423639×10^{-10}	5.423640×10^{-10}
	-0.5	0.674104	0.674104	0.671662	0.671662	0.671662	8.942070×10^{-10}	8.942071×10^{-10}
0.1	0.0	1.111410	1.111410	1.107380	1.107380	1.107380	1.474298×10^{-9}	1.474298×10^{-9}
	0.5	1.832410	1.832410	1.825770	1.825770	1.825770	2.430706×10^{-9}	2.430706×10^{-9}
	1.0	3.021130	3.021130	3.010180	3.010180	3.010180	4.007557×10^{-9}	4.007558×10^{-9}
	-1.0	0.412638	0.412638	0.410656	0.410656	0.410656	6.793135×10^{-8}	6.793135×10^{-8}
	-0.5	0.680325	0.680325	0.677057	0.677057	0.677057	1.119998×10^{-7}	1.119998×10^{-7}
0.5	0.0	1.121670	1.121670	1.116280	1.116280	1.116280	1.846565×10^{-7}	1.846565×10^{-7}
	0.5	1.849320	1.849320	1.840430	1.840430	1.840430	3.044472×10^{-7}	3.044472×10^{-7}
	1.0	3.049010	3.049010	3.034360	3.034360	3.034360	5.019485×10^{-7}	5.019485×10^{-7}
	-1.	0.4158180	0.415818	0.414782	0.414782	0.414783	5.448142×10^{-7}	5.448142×10^{-7}
	-0.5	0.685568	0.685568	0.683861	0.683861	0.683861	8.982467×10^{-7}	8.982467×10^{-7}
1.0	0.0	1.130310	1.130310	1.127500	1.127500	1.127500	1.480958×10^{-6}	1.480958×10^{-6}
	0.5	1.863570	1.863570	1.858930	1.858930	1.858930	2.441687×10^{-6}	2.441687×10^{-6}
	1.0	3.072500	3.072500	3.064850	3.064850	3.064850	4.025662×10^{-6}	4.025662×10^{-6}

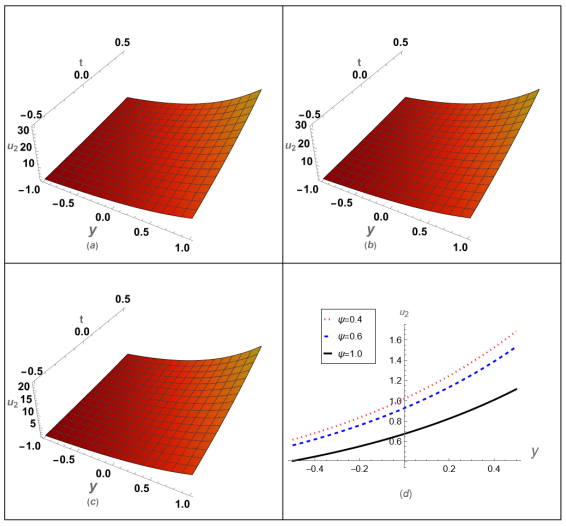

Figure 4: Effect of fractional order, (a) $\psi = 0.4$, (b) $\psi = 0.6$, (c) $\psi = 1.0$ on the approximate solution and (d) comparison of fractional order ψ of the solution $u_2(y, z, t)$ at $t = 1$, $\hbar = -1$, and $z = 0.1$.

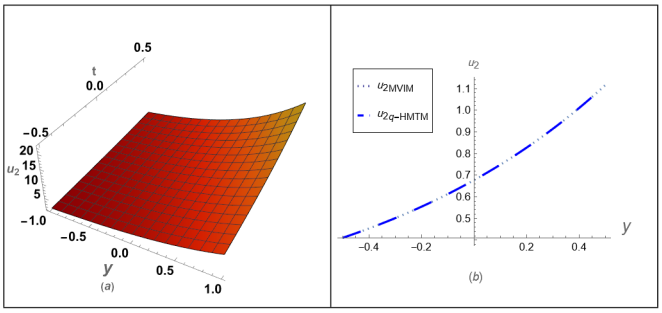

Figure 5: Comparison among MVIM solution and q-HMTM solution $u_2(y, z, t)$ at $t = 1$, $\hbar = -1$, and $z = 0.1$.

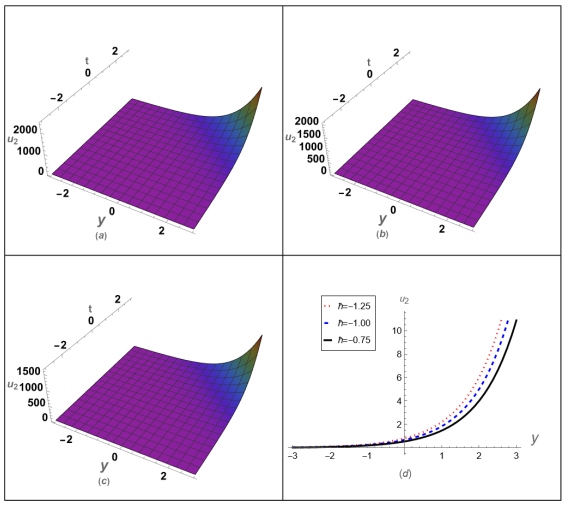

Figure 6: Effect of the auxiliary parameter, (a) $\hbar = -1.25$; (b) $\hbar = -1$; (c) $\hbar = -0.75$ on the approximate solution $u_2(y, z, t)$ at $t = 1$ and $z = 0.1$.

5. Numerical example 2

5.1. *Utilization of* q-*HMTM*

Assume the NS equation of time fractional order:

$$\begin{aligned} D_t^{\psi} u_1 - a\frac{\partial^2 u_1}{\partial y^2} - a\frac{\partial^2 u_1}{\partial z^2} + u_2\frac{\partial u_1}{\partial z} + u_1\frac{\partial u_1}{\partial y} - q = 0, \\ D_t^{\psi} u_2 - a\frac{\partial^2 u_2}{\partial y^2} - a\frac{\partial^2 u_2}{\partial z^2} + u_1\frac{\partial u_2}{\partial y} + u_2\frac{\partial u_2}{\partial z} + q = 0, \end{aligned} \tag{5.1}$$

where $0 < \psi \leqslant 1$. IC's are given as:

$$u_1(y,z,0) = -\sin(y+z),$$
$$u_2(y,z,0) = \sin(y+z),$$
$$\mathcal{M}[u_1] - s\,(\sin(y+z)) + \frac{1}{s^\psi}\mathcal{M}\Big[-a\frac{\partial^2 u_1}{\partial y^2} - a\frac{\partial^2 u_1}{\partial z^2} + u_2\frac{\partial u_1}{\partial z} + u_1\frac{\partial u_1}{\partial y} - q\Big] = 0,$$
$$\mathcal{M}[u_2] + s\,(\sin(y+z)) + \frac{1}{s^\psi}\mathcal{M}\Big[-a\frac{\partial^2 u_2}{\partial y^2} - a\frac{\partial^2 u_2}{\partial z^2} + u_1\frac{\partial u_2}{\partial y} + u_2\frac{\partial u_2}{\partial z} + q\Big] = 0.$$

The non-linear operator is defined as:

$$\begin{aligned}
&\mathcal{N}^1[\varphi_1(y,z,t;q), \varphi_2(y,z,t;q)] \\
&\quad = \mathcal{M}[\varphi_1(y,z,t;q)] - s\,(\sin(y+z)) + \frac{1}{s^\psi}\mathcal{M}\Big[-a\frac{\partial^2 \varphi_1(y,z,t;q)}{\partial y^2} \\
&\qquad - a\frac{\partial^2 \varphi_1(y,z,t;q)}{\partial z^2} + \varphi_2(y,z,t;q)\frac{\partial \varphi_1(y,z,t;q)}{\partial z} + \varphi_1(y,z,t;q)\frac{\partial \varphi_1(y,z,t;q)}{\partial y} - q\Big], \\
&\mathcal{N}^2[\varphi_1(y,z,t;q), \varphi_2(y,z,t;q)] \\
&\quad = \mathcal{M}[\varphi_2(y,z,t;q)] + s\,(\sin(y+z)) + \frac{1}{s^\psi}\mathcal{M}\Big[-a\frac{\partial^2 \varphi_2(y,z,t;q)}{\partial y^2} \\
&\qquad - a\frac{\partial^2 \varphi_2(y,z,t;q)}{\partial z^2} + \varphi_1(y,z,t;q)\frac{\partial \varphi_2(y,z,t;q)}{\partial y} + \varphi_2(y,z,t;q)\frac{\partial \varphi_2(y,z,t;q)}{\partial z} + q\Big].
\end{aligned}$$

The Mohand operator is defined as:

$$\mathcal{M}[u_{1m} - k_m u_{1m-1}] = \hbar\, \mathfrak{h}(y,z,t)\mathcal{R}_{1,m}[\overrightarrow{u_1}_{m-1}, \overrightarrow{u_2}_{m-1}],$$
$$\mathcal{M}[u_{2m} - k_m u_{2m-1}] = \hbar\, \mathfrak{h}(y,z,t)\mathcal{R}_{2,m}[\overrightarrow{u_1}_{m-1}, \overrightarrow{u_2}_{m-1}].$$

Here,

$$\begin{aligned}
&\mathcal{R}_{1,m}[\overrightarrow{u_1}_{m-1}, \overrightarrow{u_2}_{m-1}] \\
&\quad = \mathcal{M}[u_{1m-1}] - s\left(1 - \frac{k_m}{n}\right)(\sin(y+z)) + \frac{1}{s^\psi}\mathcal{M}\Big[-a\frac{\partial^2 u_{1m-1}}{\partial y^2} \\
&\qquad - a\frac{\partial^2 u_{1m-1}}{\partial z^2} + \sum_{i=0}^{m-1} u_{2i}\frac{\partial u_{1m-1-i}}{\partial z} + \sum_{i=0}^{m-1} u_{1i}\frac{\partial u_{1m-1-i}}{\partial y} - q\Big], \\
&\mathcal{R}_{2,m}[\overrightarrow{u_1}_{m-1}, \overrightarrow{u_2}_{m-1}] \\
&\quad = \mathcal{M}[u_{2m-1}] + s\left(1 - \frac{k_m}{n}\right)(\sin(y+z)) + \frac{1}{s^\psi}\mathcal{M}\Big[-a\frac{\partial^2 u_{2m-1}}{\partial y^2} \\
&\qquad - a\frac{\partial^2 u_{2m-1}}{\partial z^2} + \sum_{i=0}^{m-1} u_{1i}\frac{\partial u_{2m-1-i}}{\partial y} + \sum_{i=0}^{m-1} u_{2i}\frac{\partial u_{2m-1-i}}{\partial z} + q\Big],
\end{aligned}$$

$$\begin{aligned}
u_{1m} &= k_m u_{1m-1} + \hbar\mathcal{M}^{-1}[\mathfrak{h}(y,z,t)\mathcal{R}_{1,m}(\overrightarrow{u_1}_{m-1}, \overrightarrow{u_2}_{m-1}), \\
u_{2m} &= k_m u_{2m-1} + \hbar\mathcal{M}^{-1}[\mathfrak{h}(y,z,t)\mathcal{R}_{2,m}(\overrightarrow{u_1}_{m-1}, \overrightarrow{u_2}_{m-1}).
\end{aligned} \tag{5.2}$$

With the help of initial condition (5.2) we obtain the subsequent outcome:

$$u_{11} = \frac{\hbar t^\psi(-2a\sin(y+z) - q)}{\Gamma(\psi+1)},$$

$$u_{21} = \frac{\hbar t^{\psi}(2a\sin(y+z)+q)}{\Gamma(\psi+1)},$$
$$u_{12} = \hbar t^{\psi}\Big(-\frac{4a^2\hbar t^{\psi}\sin(y+z)}{\Gamma(2\psi+1)} - \frac{(n+\hbar)(2a\sin(y+z)+q)}{\Gamma(\psi+1)}\Big),$$
$$u_{22} = \hbar t^{\psi}\Big(\frac{4a^2\hbar t^{\psi}\sin(y+z)}{\Gamma(2\psi+1)} + \frac{(n+\hbar)(2a\sin(y+z)+q)}{\Gamma(\psi+1)}\Big),$$

and so on. The solution of equation (5.1), as determined by q-HMTM, is as follows:

$$u_1 = u_{10} + \sum_{m=1}^{\infty} u_{1m}\left(\frac{1}{n}\right)^m, \quad u_2 = u_{20} + \sum_{m=1}^{\infty} u_{2m}\left(\frac{1}{n}\right)^m.$$

For $\psi = 1$, $\hbar = -1$, and $n = 1$ solutions $\sum_{m=1}^{N} u_{1m}\left(\frac{1}{n}\right)^m$ and $\sum_{m=1}^{N} u_{2m}\left(\frac{1}{n}\right)^m$ converge to the exact solutions as $N \to \infty$,

$$u_1(y,z,t) = -\sin(y+z) + \frac{\hbar t^{\psi}(-2a\sin(y+z)-q)}{\Gamma(\psi+1)} + \hbar t^{\psi}\Big(-\frac{4a^2\hbar t^{\psi}\sin(y+z)}{\Gamma(2\psi+1)} - \frac{(n+\hbar)(2a\sin(y+z)+q)}{\Gamma(\psi+1)}\Big) = -e^{-2at}\sin(y+z),$$
$$u_2(y,z,t) = \sin(y+z) + \frac{\hbar t^{\psi}(2a\sin(y+z)+q)}{\Gamma(\psi+1)} + \hbar t^{\psi}\Big(\frac{4a^2\hbar t^{\psi}\sin(y+z)}{\Gamma(2\psi+1)} + \frac{(n+\hbar)(2a\sin(y+z)+q)}{\Gamma(\psi+1)}\Big) = e^{-2at}\sin(y+z).$$

5.2. Utilization of MVIM

Assume the NS equation of time fractional order:

$$D_t^{\psi}u_1 = a\frac{\partial^2 u_1}{\partial y^2} + a\frac{\partial^2 u_1}{\partial z^2} - u_2\frac{\partial u_1}{\partial z} - u_1\frac{\partial u_1}{\partial y} - q, \quad D_t^{\psi}u_2 = a\frac{\partial^2 u_2}{\partial y^2} + a\frac{\partial^2 u_2}{\partial z^2} - u_1\frac{\partial u_2}{\partial y} - u_2\frac{\partial u_2}{\partial z} + q, \quad (5.3)$$

where $0 < \psi \leqslant 1$. IC's are given as $u_1(y,z,0) = -\sin(y+z)$, $u_2(y,z,0) = \sin(y+z)$. Using the iterative formula found in equation (3.9), we can obtain

$$u_{1n+1} = u_{1n} + \mathcal{M}^{-1}\Big[\frac{1}{s^{\psi}}\sum_{k=0}^{m-1} s^{\psi-k-1}\frac{\partial^k u_1(y,z,0)}{\partial t^k} + \mathcal{M}[a\frac{\partial^2 u_{1n}}{\partial y^2} + a\frac{\partial^2 u_{1n}}{\partial z^2} - u_{2n}\frac{\partial u_{1n}}{\partial z} - u_{1n}\frac{\partial u_{1n}}{\partial y} - q]\Big],$$
$$u_{2n+1} = u_{2n} + \mathcal{M}^{-1}\Big[\frac{1}{s^{\psi}}\sum_{k=0}^{m-1} s^{\psi-k-1}\frac{\partial^k u_2(y,z,0)}{\partial t^k} + \mathcal{M}[a\frac{\partial^2 u_{2n}}{\partial y^2} + a\frac{\partial^2 u_{2n}}{\partial z^2} - u_{1n}\frac{\partial u_{2n}}{\partial y} - u_{2n}\frac{\partial u_{2n}}{\partial z} + q]\Big].$$

Inserting $n = 0$ into the expression above results in the second approximation we have

$$u_{11} = u_{10} + \mathcal{M}^{-1}\Big[\frac{1}{s^{\psi}}\sum_{k=0}^{m-1} s^{\psi-k-1}\frac{\partial^k u_1(y,z,0)}{\partial t^k} + \mathcal{M}[a\frac{\partial^2 u_{10}}{\partial y^2} + a\frac{\partial^2 u_{10}}{\partial z^2} - u_{20}\frac{\partial u_{10}}{\partial z} - u_{10}\frac{\partial u_{10}}{\partial y} - q]\Big],$$
$$u_{21} = u_{20} + \mathcal{M}^{-1}\Big[\frac{1}{s^{\psi}}\sum_{k=0}^{m-1} s^{\psi-k-1}\frac{\partial^k u_2(y,z,0)}{\partial t^k} + \mathcal{M}[a\frac{\partial^2 u_{20}}{\partial y^2} + a\frac{\partial^2 u_{20}}{\partial z^2} - u_{10}\frac{\partial u_{20}}{\partial y} - u_{20}\frac{\partial u_{20}}{\partial z} + q]\Big].$$

By simplification, we get

$$u_{11} = \frac{\sin(y+z)\left(2at^{\psi} - \Gamma(\psi+1)\right) + qt^{\psi}}{\Gamma(\psi+1)}, \quad u_{21} = \frac{\sin(y+z)\left(\Gamma(\psi+1) - 2at^{\psi}\right) - qt^{\psi}}{\Gamma(\psi+1)}.$$

By taking $n = 1$, we have

$$u_{12} = u_{11} + \mathcal{M}^{-1}\Big[\frac{1}{s^{\psi}}\sum_{k=0}^{m-1} s^{\psi-k-1}\frac{\partial^k u_1(y,z,0)}{\partial t^k} + \mathcal{M}[a\frac{\partial^2 u_{11}}{\partial y^2} + a\frac{\partial^2 u_{11}}{\partial z^2} - u_{21}\frac{\partial u_{11}}{\partial z} - u_{11}\frac{\partial u_{11}}{\partial y} - q]\Big],$$

$$u_{22} = u_{21} + \mathcal{M}^{-1}\Big[\frac{1}{s^{\psi}}\sum_{k=0}^{m-1} s^{\psi-k-1}\frac{\partial^k u_2(y,z,0)}{\partial t^k} + \mathcal{M}[a\frac{\partial^2 u_{21}}{\partial y^2} + a\frac{\partial^2 u_{21}}{\partial z^2} - u_{11}\frac{\partial u_{21}}{\partial y} - u_{21}\frac{\partial u_{21}}{\partial z} + q]\Big].$$

By simplifying the expression, we achieve the subsequent final outcome.

$$u_{12}(y,z,t) = -\sin(y+z) + \frac{2at^{\psi}\sin(y+z)}{\Gamma(\psi+1)} + \frac{qt^{\psi}}{\Gamma(\psi+1)} - \frac{4a^2t^{2\psi}\sin(y+z)}{\Gamma(2\psi+1)},$$

$$u_{22}(y,z,t) = \sin(y+z) - \frac{2at^{\psi}\sin(y+z)}{\Gamma(\psi+1)} - \frac{qt^{\psi}}{\Gamma(\psi+1)} + \frac{4a^2t^{2\psi}\sin(y+z)}{\Gamma(2\psi+1)},$$

Table 3: q-HMTM and MVIM solution error comparison of $u_1(y,z,t)$ at $z = 0.1$ and $\hbar = -1$.

t	y	MVIM$_{\psi=0.6}$	q-HMTM$_{\psi=0.6}$	MVIM$_{\psi=1}$	q-HMTM$_{\psi=1}$	Exact	MVIM Error$_{\psi=1}$	q-HMTM Error$_{\psi=1}$
	-1.0	0.778941	0.778941	0.781762	0.781762	0.781762	1.043913×10^{-9}	1.043913×10^{-9}
	-0.5	0.387238	0.387238	0.388640	0.388640	0.388640	5.189649×10^{-10}	5.189649×10^{-10}
0.1	0.0	-0.099274	-0.099274	-0.099633	-0.099633	-0.099633	1.330447×10^{-10}	1.330446×10^{-10}
	0.5	-0.561481	-0.561481	-0.563514	-0.563514	-0.563514	7.524804×10^{-10}	7.524803×10^{-10}
	1.0	-0.886217	-0.886217	-0.889427	-0.889427	-0.889427	1.187682×10^{-9}	1.187682×10^{-9}
	-1.0	0.771883	0.771883	0.775533	0.775533	0.775533	1.302287×10^{-7}	1.302287×10^{-7}
	-0.5	0.383729	0.383729	0.385544	0.385544	0.385544	6.474112×10^{-8}	6.474112×10^{-8}
0.5	0.0	-0.098374	-0.098374	-0.098840	-0.098840	-0.098840	1.659738×10^{-8}	1.659738×10^{-8}
	0.5	-0.556393	-0.556393	-0.559024	-0.559024	-0.559024	9.387228×10^{-8}	9.387228×10^{-8}
	1.0	-0.878187	-0.878187	-0.882340	-0.882340	-0.882340	1.481639×10^{-7}	1.481639×10^{-7}
	-1.0	0.766078	0.7660780	0.767817	0.767817	0.767816	1.039234×10^{-6}	1.039234×10^{-6}
	-0.5	0.380843	0.3808430	0.381708	0.381708	0.381707	5.166386×10^{-7}	5.166386×10^{-7}
1.0	0.0	-0.097635	-0.097635	-0.097856	-0.097856	-0.097856	1.324483×10^{-7}	1.324483×10^{-7}
	0.5	-0.552209	-0.552209	-0.553463	-0.553463	-0.553462	7.491073×10^{-7}	7.491073×10^{-7}
	1.0	-0.871583	-0.871583	-0.873561	-0.873561	-0.873560	1.182358×10^{-6}	1.182358×10^{-6}

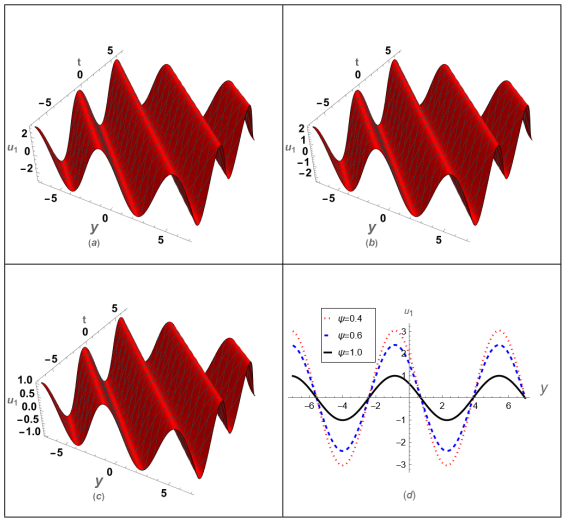

Figure 7: Effect of fractional order, (a) $\psi = 0.4$; (b) $\psi = 0.6$; (c) $\psi = 1.0$ on the approximate solution; and (d) comparison of fractional order ψ of the solution $u_1(y,z,t)$ at $t = 1$, $\hbar = -1$, and $z = 0.1$.

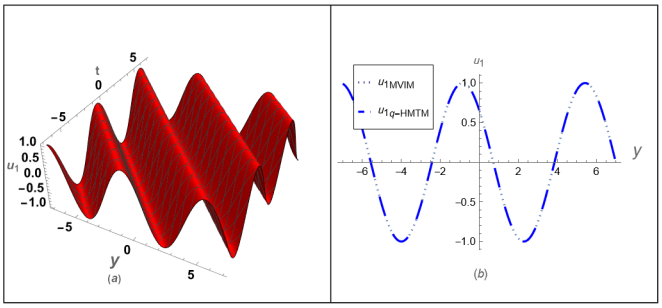

Figure 8: Comparison among MVIM and q-HMTM solution $u_1(y,z,t)$ at $t=1$, $\hbar=-1$, and $z=0.1$.

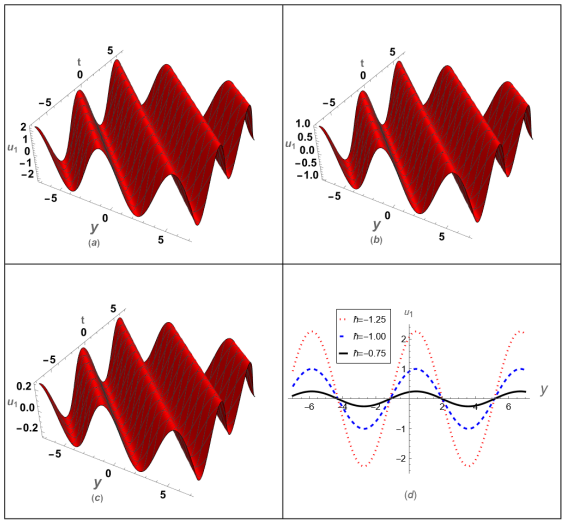

Figure 9: Effect of the auxiliary parameter, (a) $\hbar=-1.25$; (b) $\hbar=-1$; (c) $\hbar=-0.75$ on the approximate solution $u_1(y,z,t)$ at $t=1$ and $z=0.1$.

Table 4: q-HMTM and MVIM solution error comparison of $u_2(y,z,t)$ at $z=0.1$ and $\hbar=-1$.

t	y	MVIM$_{\psi=0.6}$	q-HMTM$_{\psi=0.6}$	MVIM$_{\psi=1}$	q-HMTM$_{\psi=1}$	Exact	MVIM Error$_{\psi=1}$	q-HMTM Error$_{\psi=1}$
	-1.0	-0.778941	-0.778941	-0.781762	-0.781762	-0.781762	1.043913×10^{-9}	1.043913×10^{-9}
	-0.5	-0.387238	-0.387238	-0.388640	-0.388640	-0.388640	5.189649×10^{-10}	5.189649×10^{-10}
0.1	0.0	0.099274	0.099274	0.099633	0.099633	0.099633	1.330446×10^{-10}	1.330446×10^{-10}
	0.5	0.561481	0.561481	0.563514	0.563514	0.563514	7.524803×10^{-10}	7.524803×10^{-10}
	1.0	0.886217	0.886217	0.889427	0.889427	0.889427	1.187682×10^{-9}	1.187682×10^{-9}
	-1.0	-0.771883	-0.771883	-0.775533	-0.775533	-0.775533	1.302287×10^{-7}	1.302287×10^{-7}
	-0.5	-0.383729	-0.383729	-0.385544	-0.385544	-0.385544	6.474112×10^{-8}	6.474112×10^{-8}
0.5	0.0	0.098374	0.098374	0.098840	0.098840	0.098840	1.659738×10^{-8}	1.659738×10^{-8}
	0.5	0.556393	0.556393	0.559024	0.559024	0.559024	9.387228×10^{-8}	9.387228×10^{-8}
	1.0	0.878187	0.878187	0.882340	0.882340	0.882340	1.481639×10^{-7}	1.481639×10^{-7}
	-1.0	-0.766078	-0.766078	-0.767817	-0.767817	-0.767816	1.039234×10^{-6}	1.039234×10^{-6}
	-0.5	-0.380843	-0.380843	-0.381708	-0.381708	-0.381707	5.166386×10^{-7}	5.166386×10^{-7}
1.0	0.0	0.097635	0.097635	0.097856	0.097856	0.097856	1.324483×10^{-7}	1.324483×10^{-7}
	0.5	0.552209	0.552209	0.553463	0.553463	0.553462	7.491073×10^{-7}	7.491073×10^{-7}
	1.0	0.871583	0.871583	0.873561	0.873561	0.873560	1.182358×10^{-6}	1.182358×10^{-6}

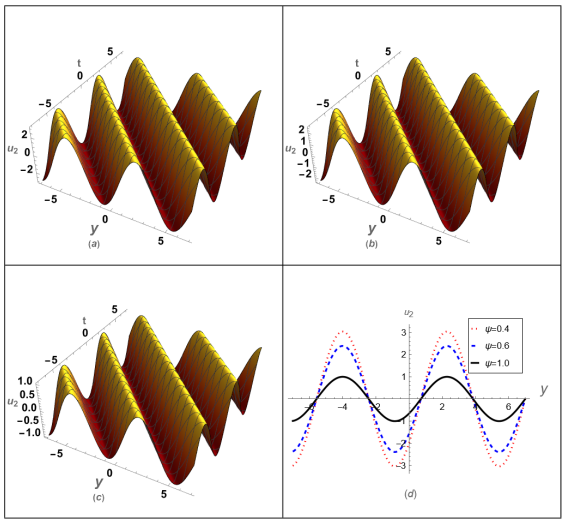

Figure 10: Effect of fractional order, (a) $\psi = 0.4$; (b) $\psi = 0.6$; (c) $\psi = 1.0$ on the approximate solution; and (d) comparison of fractional order ψ of the solution $u_2(y, z, t)$ at $t = 1$, $\hbar = -1$, and $z = 0.1$.

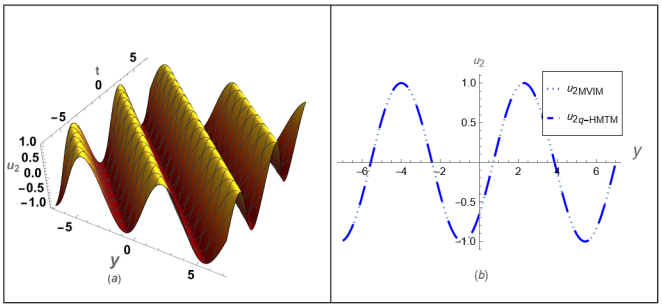

Figure 11: Comparison among MVIM solution and q-HMTM solution $u_2(y, z, t)$ at $t = 1$, $\hbar = -1$, and $z = 0.1$.

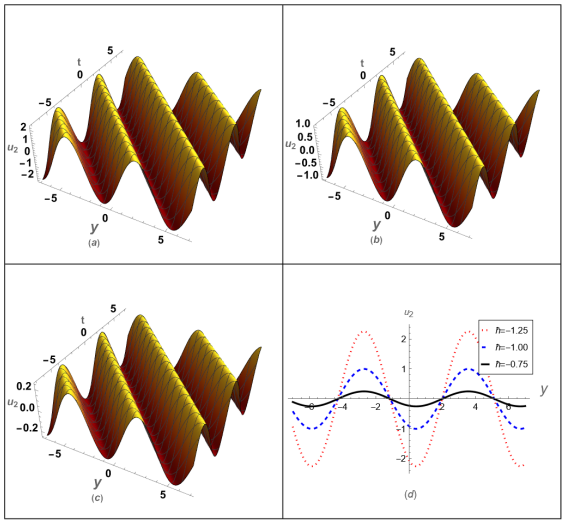

Figure 12: Effect of the auxiliary parameter, (a) $\hbar = -1.25$; (b) $\hbar = -1$; (c) $\hbar = -0.75$ on the approximate solution $u_2(y, z, t)$ at $t = 1$ and $z = 0.1$.

6. Result and discussion

The numerical studies illustrated in Tables 1-4 and Figures 1-11 form a thorough comparison between the two methods, the MVIM, and the q-HMTM in solving the time-fractional NS equations under two different sets of initial conditions. Both methods are very accurate in all the test cases, it is clear that the absolute errors are extremely small. This proves both approaches to be efficient and reliable in solving

problems of fractional fluid dynamics.

The numerical result of u_1 and u_2 determined using MVIM and q-HMTM in the case of Problem 1 are given in the Tables 1-2 are quite near to the exact solution. The absolute errors in the case of $\psi = 1$ are small at all-time levels, which means that the approximation is numerically stable and quite precise. Referring to Figures 1 and 4 we noticed that the profiles of the solutions are highly affected by the fractional order ψ in the sense that as ψ deviates and moves from the value of 0.4 to 1.0, the solutions start showing reduction in memory effect and converging to their classical integer-order counterparts. This fact is further indicated by the dominance of the time curves generated by MVIM and q-HMTM shown in Figures 2 and 5, which are approximately same, expressing the harmony of the two methods.

Similarly for Problem 2 the values of u_1 and u_2 determined using MVIM and q-HMTM are given in the Tables 3-4, in this case the sinusoidal initial conditions are used. Absolute errors of the two methods are both in the negligible level and have close concurrence with the exact solutions. In Figures 7 and 10, the obvious role of the fractional order is once more demonstrated: the lower ψ lead to the slower diffusion and more oscillatory dynamics, whereas $\psi = 1$ results in smoother profiles that resemble NS dynamics. Comparisons in Figures 8 and 11 prove that q-HMTM is slightly faster in converging without affecting numerical stability in comparison with MVIM.

The auxiliary parameter $\hbar$ is very important in regulating convergence and accuracy of approximate solutions to q-HMTM. The effect of varying values of $\hbar$ (i.e., $\hbar$= -0.75,-1,-1.25) on solutions u_1 and u_2 at $t = 1$ and $z = 0.1$ is clearly shown in Figures 3, 6, 9, and 12. The difference between the curves of the solutions is noted to be altered by changing the auxiliary parameter in terms of shape and amplitude. As an example, by setting $\hbar = -1.25$, the solution will have some greater deviations whereas $\hbar = -0.75$ will have smoother curves. The case $\hbar = -1$ seems to provide a more symmetric and stable profile and better convergence properties and compatibility with the expected results of the fractional-order NS system. This also shows that $\hbar$ can be viewed as convergence-control parameter where one can be flexible to modify the approximation based on the kind of nonlinear fractional model of interest. Reasonable choice of $\hbar$ is thus key to resolving correct and stable solutions, and the given graphical data explains that the given q-HMTM indeed offers a successful platform to make such adjustment.

The results also highlight the physical significance of fractional-order effects in fluid dynamics. Variations in ψ directly influence the evolution of the flow field: smaller values of ψ enhance memory effects, leading to slower decay of vorticity and more sustained flow structures, while larger values reduce these effects, approaching the behavior of the classical NS model. This adaptability allows the fractional-order NS equations to model a wider spectrum of fluid phenomena, including anomalous diffusion in porous media and the complex decay behavior in viscoelastic or turbulent flows. The combined application of the Mohand transformation, with its computational advantages over other transforms, and the convergence control offered by $\hbar = -1$ in the q-HMTM framework therefore provides a powerful and precise approach for exploring such fractional-order fluid systems.

7. Conclusion

In this paper, the time-fractional NS equations were solved effectively by using MVIM and q-HMTM. These findings were verified together with precisely determined solutions to show that both methods give outstanding precision and negligible errors even in the case of nonlinear coupled systems. Combination of the Mohand transformation with q-HAM and VIM framework was quite effective to not only result in significantly faster convergence and stability but also effective in preserving the non-trivial memory effects exhibited by fractional-order models. The Mohand transformation also proved to be more simple, efficient and robust in terms of computational advantage, in comparison with other methods of fractional operator transformation, especially with respect to multi-term fractional operators. Furthermore, the dependence of the fractional order ψ showed that it has a significant effect on the behavior of the fluid that is flexible enough to explain the classic as well as the anomalous transport processes. In general, the synergistic combination of the Mohand transformation with q-HAM and VIM offers both a robust

and elegantly concise method of performing accurate and precise analytical studies of complex fractional fluid dynamics processes, promising future opportunities to explore advanced fluid dynamics as well as in practical applications.

Acknowledgment

The authors gratefully acknowledge the referees for their insightful comments and suggestions. They also extend their appreciation to the Public Authority for Applied Education and Training (PAAET) for supporting this research through project number BE-25-01.

References

[1] S. Abuasad, I. Hashim, *Homotopy decomposition method for solving one-dimensional time-fractional diffusion equation*, AIP Conf. Proc., **1940** (2018), 1–6. 1
[2] S. Abuasad, I. Hashim, *Homotopy decomposition method for solving higher-order time-fractional diffusion equation via modified beta derivative*, Sains Malays., **47** (2018), 2899–2905. 1
[3] S. Abuasad, A. Yildirim, I. Hashim, S. A. Abdul Karim, J. F. Gomez-Aguilar, *Fractional multi-step differential transformed method for approximating a fractional stochastic SIS epidemic model with imperfect vaccination*, Int. J. Environ. Res. Public Health, **16** (2019), 15 pages. 1
[4] J. Adams, W. Harris, G. Jenkins, R. Parker, L. Wright, *A study of the differences and similarities between Mohand and Elzaki transforms*, **15** (2024), 17–26. 1
[5] G. Adomian, *Solving frontier problems of physics: the decomposition method*, Kluwer Academic Publishers Group, Dordrecht, (1994). 1
[6] S. Aggarwal, R. Chaudhary, *A comparative study of Mohand and Laplace transforms*, J. Emerg. Technol. Innov. Res., **6** (2019), 230–240. 1
[7] S. Aggarwal, R. Chauhan, *A comparative study of Mohand and Aboodh transforms*, Int. J. Res. Advent Technol., **7** (2019), 520–529.
[8] S. Aggarwal, A. R. Gupta, *Dualities between Mohand transform and some useful integral transforms*, Int. J. Recent Technol. Eng., **8** (2019), 843–847.
[9] S. Aggarwal, S. D. Sharma, *A comparative study of Mohand and Sumudu transforms*, J. Emerg. Technol. Innov. Res., **6** (2019), 145–153. 1
[10] A. A. Alderremy, R. Shah, N. A. Shah, S. Aly, K. Nonlaopon, *Comparison of two modified analytical approaches for the systems of time fractional partial differential equations*, AIMS Math., **8** (2023), 7142–7162. 1
[11] N. Anjum, J.-H. He, *Laplace transform: making the variational iteration method easier*, Appl. Math. Lett., **92** (2019), 134–138. 1
[12] D. Baleanu, Z. B. Güvenç, J. A. Tenreiro Machado, *New trends in nanotechnology and fractional calculus applications*, Springer, New York, (2010). 1
[13] D. Baleanu, G.-C. Wu, S.-D. Zeng, *Chaos analysis and asymptotic stability of generalized Caputo fractional differential equations*, Chaos Solitons Fractals, **102** (2017), 99–105. 1
[14] G. A. Birajdar, *Numerical solution of time-fractional Navier-Stokes equation by discrete Adomian decomposition method*, Nonlinear Eng., **3** (2014), 21–26. 1
[15] A. Bokhari, *Application of Shehu transform to Atangana-Baleanu derivatives*, J. Math. Comput. Sci., **20** (2019), 101–107. 1
[16] H. Bulut, T. A. Sulaiman, H. M. Baskonus, H. Rezazadeh, M. Eslami, M. Mirzazadeh, *Optical solitons and other solutions to the conformable space-time fractional Fokas-Lenells equation*, Optik, **172** (2018), 20–27. 1
[17] V. B. L. Chaurasia, D. Kumar, *Solution of the time-fractional Navier-Stokes equation*, Gen. Math. Notes, **4** (2011), 49–59. 1
[18] M. Dehghan, *Finite difference procedures for solving a problem arising in modeling and design of certain optoelectronic devices*, Math. Comput. Simul., **71** (2006), 16–30. 1
[19] M. El-Shahed, A. Salem, *On the generalized Navier-Stokes equations*, Appl. Math. Comput., **156** (2004), 287–293. 1
[20] Z. Z. Ganji, D. D. Ganji, A. D. Ganji, M. Rostamian, *Analytical solution of time-fractional Navier-Stokes equation in polar coordinate by homotopy perturbation method*, Numer. Methods Partial Differ. Equ., **26** (2010), 117–124. 1
[21] J. H. He, *Approximate solution of nonlinear differential equations with convolution product nonlinearities*, Comput. Methods Appl. Mech. Eng., **167** (1998), 69–73. 1
[22] J.-H. He, *Variational iteration method for autonomous ordinary differential systems*, Appl. Math. Comput., **114** (2000), 115–123. 1
[23] R. Herrmann, *Fractional calculus: an introduction for physicists*, World Scientific, Singapore, (2011). 1
[24] R. Hilfer, *Applications of fractional calculus in physics*, World Scientific, Singapore, (2000). 1
[25] H. Jafari, *A new general integral transform for solving integral equations*, J. Adv. Res., **32** (2021), 133–138. 2.4

[26] A. Khalouta, A. Kadem, *A new method to solve fractional differential equations: inverse fractional Shehu transform method*, Appl. Appl. Math., **14** (2019), 926–941. 1
[27] A. A. Kilbas, H. M. Srivastava, J. J. Trujillo, *Theory and applications of fractional differential equations*, Elsevier Science B.V., Amsterdam, (2006). 1
[28] S. Kumar, D. Kumar, S. Abbasbandy, M. M. Rashidi, *Analytical solution of fractional Navier-Stokes equation by using modified Laplace decomposition method*, Ain Shams Eng. J., **5** (2014), 569–574. 1
[29] D. Kumar, J. Singh, S. Kumar, *A fractional model of Navier-Stokes equation arising in unsteady flow of a viscous fluid*, J. Assoc. Arab Univ. Basic Appl. Sci., **17** (2015), 14–19. 1
[30] M. I. Liaqat, A. Khan, M. A. Alqudah, T. Abdeljawad, *Adapted homotopy perturbation method with Shehu transform for solving conformable fractional nonlinear partial differential equations*, Fractals, **31** (2023), 19 pages. 1
[31] J. Liouville, *Second memoire sur le developpement des fonctions ou parties de fonctions en series dont les divers termes sont assujettis a satisfaire a une meme equation differentielle du second ordre, contenant un parametre variable*, J. Math. Pure et Appl., **2** (1837), 16–35. 1
[32] Y. Liu, K. D. Xu, J. Li, Y. J. Guo, A. Zhang, Q. Chen, *Millimeter-wave E-plane waveguide bandpass filters based on spoof surface plasmon polaritons*, IEEE Trans. Microw. Theory Tech., **70** (2022), 4399–4409. 1
[33] K. Liu, Z. Yang, W. Wei, B. Gao, D. Xin, C. Sun, G. Gao, G. Wu, *Novel detection approach for thermal defects: Study on its feasibility and application to vehicle cables*, High Voltage, **8** (2023), 358–367. 1
[34] L. Liu, L. Zhang, G. Pan, S. Zhang, *Robust yaw control of autonomous underwater vehicle based on fractional-order PID controller*, Ocean Eng., **257** (2022). 1
[35] K. S. Miller, B. Ross, *Fractional difference calculus*, In: Univalent functions, fractional calculus, and their applications, Horwood, Chichester, (1989), 139–152. 1
[36] M. Mohand, A. Mahgoub, *The new integral transform "Mohand Transform"*, Adv. Theor. Appl. Math., **12** (2017), 113–120. 2.1
[37] S. Momani, Z. Odibat, *Analytical solution of a time-fractional Navier-Stokes equation by Adomian decomposition method*, Appl. Math. Comput., **177** (2006), 488–494. 1
[38] M. Nadeem, J.-H. He, A. Islam, *The homotopy perturbation method for fractional differential equations: Part 1 Mohand transform*, Int. J. Numer. Methods Heat Fluid Flow, **31** (2021), 3490–3504. 2.2
[39] K. Oldham, J. Spanier, *The fractional calculus: theory and applications of differentiation and integration to arbitrary order*, Academic Press, New York, (1974). 1
[40] I. Podlubny, *Fractional differential equations*, Academic Press, San Diego, CA, (1999). 1
[41] D. G. Prakasha, P. Veeresha, H. M. Baskonus, *Analysis of the dynamics of hepatitis E virus using the Atangana-Baleanu fractional derivative*, Eur. Phys. J. Plus, **134** (2019), 1–11. 1
[42] A. Prakash, P. Veeresha, D. G. Prakasha, M. Goyal, *A new efficient technique for solving fractional coupled Navier-Stokes equations using q-homotopy analysis transform method*, Pramana – J. Phys., **93** (2019), 1–10. 1
[43] A. A. Ragab, K. M. Hemida, M. S. Mohamed, M. A. Abd El Salam, *Solution of time-fractional Navier-Stokes equation by using homotopy analysis method*, Gen. Math. Notes, **13** (2012), 13–21. 1
[44] B. Ross, *A brief history and exposition of the fundamental theory of fractional calculus*, In: Fractional Calculus and Its Applications, Springer, Berlin, (2006), 1–36. 1
[45] R. Saadeh, A. A. Alshawabkeh, R. Khalil, M. A. Abdoon, N. E. Taha, D. K. Almutairi, *The Mohand transforms and their applications for solving systems of differential equations*, Eur. J. Pure Appl. Math., **17** (2024), 385–409. 1
[46] S. G. Samko, A. A. Kilbas, O. I. Marichev, *Fractional integrals and derivatives*, Gordon and Breach Science Publishers, Yverdon, (1993). 1
[47] P. Sunthrayuth, R. Ullah, A. Khan, R. Shah, J. Kafle, I. Mahariq, F. Jarad, *Numerical analysis of the fractional-order nonlinear system of Volterra integro-differential equations*, J. Funct. Spaces, **2021** (2021), 10 pages. 1
[48] N. H. Sweilam, M. M. Abou Hasan, D. Baleanu, *New studies for general fractional financial models of awareness and trial advertising decisions*, Chaos Solitons Fractals, **104** (2017), 772–784. 1
[49] P. Veeresha, D. G. Prakasha, *Solution for fractional Zakharov-Kuznetsov equations by using two reliable techniques*, Chinese J. Phys., **60** (2019), 313–330. 1
[50] Y. Wang, X. Han, S. Jin, *MAP based modeling method and performance study of a task offloading scheme with time-correlated traffic and VM repair in MEC systems*, Wireless Netw., **29** (2023), 47–68. 1
[51] G.-C. Wu, D. Baleanu, *Variational iteration method for fractional calculus—a universal approach by Laplace transform*, Adv. Differ. Equ., **2013** (2013), 9 pages. 1
[52] Y. Xi, W. Jiang, K. Wei, T. Hong, T. Cheng, S. Gong, *Wideband RCS reduction of microstrip antenna array using coding metasurface with low Q resonators and fast optimization method*, IEEE Antennas Wirel. Propag. Lett., **21** (2021), 656–660. 1